LISA L3 gravity wave observatory: Non-linear modelling and possible DFAC methods

(Article begins on next page)

28 April 2024

IAC-18,C1,6,4,x47173

LISA L3 GRAVITY WAVE OBSERVATORY: NON-LINEAR MODELLING AND POSSIBLE DFAC METHODS

L. Colangelo[a]*, S. Vidano[a], E. Canuto[a], C. Novara[a], J. Grzymisch[b]

[a]*Department of Electronics and Telecommunications, Politecnico di Torino, Corso Duca degli Abruzzi 24, Turin 10129, Italy*, luigi.colangelo@polito.it,
[b]*Guidance, Navigation and Control Section (TEC-SAG), ESTEC, European Space Agency, Keplerlaan 1, Noordwijk 2201 AZ, The Netherlands.*
* Corresponding Author

Abstract

Recently, we witnessed the revolutionary discovery of gravitational waves (GW) by a ground-based laser interferometric observatory: a potentially game-changing observation tool in astronomy. Hence, the opportunity of setting up a space-based GW observatory, including their low-frequency spectrum not accessible from the ground, is gaining more and more support.

In this framework, the Laser Interferometer Space Antenna (LISA) mission has been already selected, within the European Space Agency selection of the L3 launch opportunity. Consequently, LISA might be the first space mission scanning the sky to retrieve both polarisations of the GWs simultaneously, and to measure their source parameters in a bandwidth spanning from 10^{-4} to 10^{-1} Hz.

The latest LISA mission concept, nominally lasting 4 years in Science Mode, encompasses three identical satellites, in an Earth-trailing heliocentric orbit about 50 Mkm from the Earth. What is more, the three satellites will be placed in a triangular constellation, whose three arms, averagely long 2.5 Mkm, are endowed with six optical links for laser interferometry. Laser interferometry aims to measure, with high accuracy, the distance variations among the free-flying test masses hosted in the three spacecrafts. To this purpose, each spacecraft is drag-free controlled, in order to follow its own two test masses, along each of its two interferometric axes.

In this paper, we first review the general aspects of the LISA mission, including those successfully tested in the LISA Pathfinder experiment. Then, an overall non-linear model is proposed to describe the LISA constellation dynamics. Possible methodologies for the LISA Drag-Free Attitude Control System (DFACS) are finally discussed.

Keywords: LISA, Gravitational waves, drag-free control, DFAC, Model-based control

Acronyms/Abbreviations

CAS Constellation Acquisition Sensor
CF Constellation Reference Frame
CoM Center of Mass
DFAC Drag-free and attitude control
DoF Degree of Freedom
EMC Embedded Model Control
EMRI Extreme Mass Ratio Inspiral
GW Gravitational waves
GWO Gravitational Waves Observatory
GRS Gravitational Reference Sensor
IF Inertial Reference Frame
ITA Inter Telescope Actuator
ITS Inter Telescope Sensor
LISA Laser Interferometric Space Antenna
LPF LISA PathFinder
LTP LISA Technology Package
MF Test Mass Reference Frame
MPS Micro Propulsion System
MPA Micro Propulsion Actuator
OA Optical Assembly
OF Optical Assembly Reference Frame
OMS Optical Metrology System

RF Reference Frame
S/C Spacecraft
SF Spacecraft Reference Frame
STR Star Trackers
TM Test Mass
w.r.t With Respect To

Mathematical notations
Main variables:

$\mathbf{r}_I$	S/C CoM position w.r.t. the IF origin - components in IF
$\mathbf{r}_M$	TM CoM position w.r.t. the cage center - components in OF
$\mathbf{r}_M^I$	TM CoM position w.r.t. the cage center - components in IF
$\mathbf{r}_{MI}$	TM CoM position w.r.t. the IF origin - components in IF
$\boldsymbol{\omega}_C$	Local constellation frame angular velocity w.r.t. IF - components in CF
$\boldsymbol{\omega}_S$	S/C angular velocity w.r.t. CF - components in SF
$\boldsymbol{\omega}_M$	TM angular velocity w.r.t OF - components in MF

$\boldsymbol{\omega}_{MI}$	TM angular velocity w.r.t IF - components in MF	$\mathbf{b}_M$	Vector from the OA pivot to the cage center - components in OF
$\boldsymbol{\theta}_S$	Euler angles of the rotation CF → SF	$\boldsymbol{\omega}_C$	CF origin angular velocity - components in CF
$\boldsymbol{\theta}_M$	Euler angles of the rotation OF → MF	K_T	TM linear stiffness matrix
$\boldsymbol{\omega}_{SI} = T_C^S \boldsymbol{\omega}_C + \boldsymbol{\omega}_S$	S/C angular velocity w.r.t. IF - components in SF	K_R	TM angular stiffness matrix
$\mathbf{p}_M(\mathbf{r}_M, \boldsymbol{\theta}_M)$	TM pose	c_{OA}	OA input coefficient

Command Inputs:

$\mathbf{F}_T(\mathbf{u}_T)$ — Commanded micro propulsion actuator (MPA) force function of the digital command $\mathbf{u}_T$ (noise is not included) - components in SF

$\mathbf{M}_T(\mathbf{u}_T)$ — Commanded MPA torque function of the digital command $\mathbf{u}_T$ (noise is not included) - components in SF

$\mathbf{F}_E(\mathbf{p}_M, \mathbf{u}_E)$ — Suspension commanded force function of the pose $\mathbf{p}_M$ and of the digital command $\mathbf{u}_E$ (noise is not included) - components in OF

$\mathbf{M}_E(\mathbf{p}_M, \mathbf{u}_E)$ — Suspension commanded torque function of the pose $\mathbf{p}_M$ and of the digital command $\mathbf{u}_E$ (noise is not included) - components in OF

u_{OA} — OA digital command

Disturbances:

$\mathbf{d}_S$ — Force acting on the S/C - components in SF

$\mathbf{D}_S$ — Moment acting on the S/C - components in SF

$\mathbf{d}_M$ — Force acting on a TM - components in OF

$\mathbf{D}_M$ — Moment acting on a TM - components in MF

Parameters:

m_S — S/C mass (including the two OAs)

m_M — TM mass

J_S — S/C inertia matrix w.r.t S/C CoM (including the two OAs and a movable antenna)

J_M — TM inertia matrix w.r.t. TM CoM

$\mu_\odot$ — Sun gravitational parameter

$\mathbf{b}_S$ — Vector from the S/C CoM to the OA pivot - components in SF

1. Introduction

The last century has seen enormous progresses in our understanding of the Universe via scientific space missions. After electromagnetic radiations, in the last years, scientists have been planning to use gravity to shed further light into the complex physics and laws behind our Universe [1]. From this perspective, gravitational waves (GWs), a sort of ripples in the fabric of space-time, are widely considered as the most effective mean to enable the scientific observation of a wide range of Universe phenomena [1].

In this framework, the Laser Interferometer Space Antenna (LISA) space mission will be paramount, since its ambitious objective of scanning the entire sky to obtain both polarisations of the GWs, while measuring source parameters with relevant sensitivity in a band from below 10^{-4} Hz to above 10^{-1} Hz.

The history of the LISA mission traces back to several years ago, and throughout the last few decades the proposed designs and architectures have been evolving, also reviewing the status of the available technology (e.g. [8], [13], [30], [31]). Recently, a new baseline architecture for the whole mission was established, as a result of trade-offs at mission and system level, encompassing three identical S/C in a triangular formation separated by 2.5 million km [1].

In parallel, the success of Lisa Pathfinder [3], [24] the ESA LISA mission precursor [25], paved the way for future missions by testing in flight some of the technologies required to enable a GWO, in space.

However, although the results and the lessons learnt from the Lisa Pathfinder mission [24], [26], will be of indisputably interest for the LISA design, some differences should be accounted for. For instance, LISA will benefit from a constellation mission scenario, and the absence of both an electrostatic suspension along the sensitive axis of the test-masses (non-coaxial TMs within the S/C) [23], [24], and the differential force effect affecting LPF results ([4], [11], [24]).

From the measurement perspective, laser interferometers are employed to measure, down to the pm level, the distance variations among the test-masses (TMs) caused by GWs. In turn, to support the GWs measurement via laser interferometry, control requirements prescribe a drag-free control of each S/C, whose telescopes must be pointed to the two other ones

(nrad DC pointing accuracy). This last objective will be enforced via the Differential Wavefront Sensing (DWS) technique, successfully flown in LPF [27], whose signals will then be used in the control system [9], [14].

In the last few years, several control architectures and methodologies have been proposed for the LISA and LISA-like missions (e.g. [1], [7], [14], [22]). In addition, the LPF precursor granted the opportunity to implement and test some of the control laws (e.g. [11], [23]), allowing control designers for a more effective refinement and tuning in view of the LISA specific objectives [4], [24], [26].

Generally speaking, the control of the three S/C to establish the GW observatory should include the constellation acquisition, the TM release, and the drag-free and attitude condition achievement, where the TMs will be in free-fall along the lines of sight between the S/C (namely, the Science Mode) [1].

By focusing on the drag-free and attitude control (DFAC) strategies, a wide range of techniques have been proposed in literature. In [7], a solution employing FEEP thrusters as actuators is proposed, while [28] leverages quantitative feedback theory to design and tune DFAC controllers. Alternatively, [22] describes the realization of a generic simulator for formation flying satellites, and the design and the application of Embedded Model Control (EMC) to the S/C constellation of drag-free satellites; a design validated by the previous GOCE mission. In [9] the performance requirements are derived from the system level requirements, while the actual design is performed, in frequency domain, by means of control system decoupling. Again in the frequency domain, [14] defines three interconnected control problems: TMs drag-free control, TMs suspension control, and S/C attitude control. Differently, in [7] and [9], the structured singular value relatively to the robust stability analysis of the LISA Science Mode is employed. [16] and [17] propose a different approach, in which sliding mode techniques are applied to the test-mass suspension control problem. Differently, [29] showed how to control LISA S/C to fly drag-free, by mitigating the effects of external disturbances with a Disturbance Reduction System (DRS) [6]. Also, an extended dynamics and control model, augmented by several internal and external disturbance sources, and a suitable controller strategy and structure, are presented in [17] and [6].

A relevant aspect in the LISA and LPF literature is the analysis of the sources of disturbances, both internal and external, affecting both the mission and platform, and potentially undermining the final scientific measurement performance (see, for instance, [3], [6], [15]). To this aim, the Science Mode, requiring near-continuous operations of the gravitational observatory system at the design sensitivity and performance, is the driving sub-scenario to be considered. As a consequence, during the Science Mode, the control system design should be such that that external perturbations are minimised.

In this paper, we first review the general aspects of the LISA mission, including those successfully tested in the LISA Pathfinder experiment. Then, an overall non-linear model is proposed to describe the LISA constellation and attitude dynamics. Possible methodologies are finally discussed, for the LISA Drag-Free Attitude Control System (DFACS), with a special attention to model-based disturbance-rejection techniques.

2. Overview of the LISA Mission

LISA will be the first space-based gravitational wave observatory (GWO) and the third ESA's large-class mission, planned for 2034. Compared to the current Earth-based GWOs, such as LIGO [20] and Virgo [21], LISA will allow observing low-frequency gravitational waves generated by merging galaxies, massive black holes and extreme mass ratio inspirals (EMRI) [1].

2.1 LISA Concept and the Pathfinder Heritage

The LISA observatory is a constellation of three spacecraft traveling on Earth-trailing heliocentric orbits at about 50 Mkm from the Earth (see Fig. 1). The orbital parameters are such that the three S/C set up a triangle with a mean side length of 2.5 Mkm. The inner angles will breath of ±1 deg, throughout the mission duration. The triangle center moves along a heliocentric orbit (1 AU radius) and has a true anomaly lower than the Earth (between 19 and 25 deg), [1].
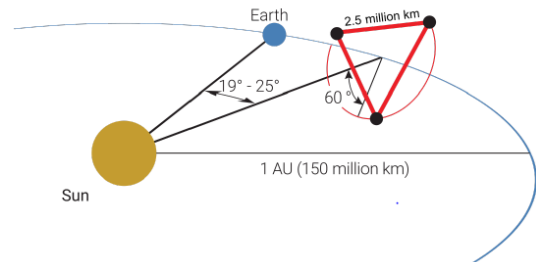

Fig. 1. LISA orbit (courtesy: [1])

The LISA spacecraft preliminary concept consists of a circular 14 m^2 solar array and a science module that contains two moving Optical Assemblies (OA): fundamental devices to establish a bidirectional laser link, within the spacecrafts. The nominal inter-angle of the two OAs is 60 deg, potentially adjustable thanks to a dedicated actuator.

In turn, each Optical Assembly is composed by: (i) a telescope, (ii) an optical bench for laser interferometry, and (iii) the Gravitational Reference Sensor (GRS). The GRS is essentially an advanced electrostatic suspension

to control and measure the attitude and position of a TM: a 1.96 kg gold-platinum cube of 46mm side, with very low magnetic susceptibility and high density to reduce the effects of external disturbances.

For what concerns other actuators and sensors, nine cold gas thrusters are arranged in three pods that are positioned 120 deg apart on the lateral surface of the science module. No reaction wheels are foreseen. Star trackers are used only for the attitude control, but not during the Science Mode since they are too noisy at low frequencies. During the Science Mode, the spacecraft attitude can be retrieved from the Optical Metrology System (OMS), which provides the horizontal/vertical tilts with respect to the incoming laser beams. The OMS is also able to provide the horizontal/vertical tilts of the test mass with respect to the laser direction. An additional sensor, the CAS, supports the constellation acquisition phase by spotting and tracking the incoming laser beam.

Due to the LISA overall complexity, ESA decided to conceive LISA Pathfinder (PF), a mid-sized precursor mission that was flown between December 2015 and June 2017. LISA PF was a technological demonstrator whose science module carried the LISA Technology Package (LTP), developed by ESA in collaboration with a consortium of European industries and research institutes. The LISA Technology Package featured the Gravitational Reference Sensor, the Optical Metrology System, the DFACS software, and the cold-gas thrusters [2]. However, test masses (TMs) were arranged and operated co-axially.

The main goals of LISA PF were to test in-flight the DFACS performances, to verify the feasibility of laser interferometry, and to test equipment in space environment. It was a successful mission with unexpected performances (e.g. the residual differential acceleration, between TMs at the end of the mission, was even lower than the LISA requirement) [3] (see Fig. 2). Moreover, LISA PF allowed to study and characterize many low-scale disturbances (e.g. the Brownian motion of residual/outgassed particles), couplings, and self-gravity effects.

Nevertheless, some relevant differences must be considered in comparing LISA mission and performance with the PF ones. In fact, LISA will require laser link acquisition and maintenance, while TMs have to be drag-free controlled on two different directions, instead of a single one. What is more, each GRS is located inside a moving telescope: a truly distinguishing configuration, whose constraints and degrees of freedom will make LISA calling for a new DFACS design.
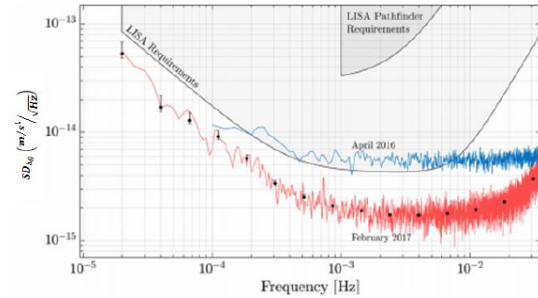

Fig. 2. LISA PF final performances (courtesy: [3])

2.2 LISA Science and AOCS Requirements

The general relativity theory states that massive bodies curve space-time and free-falling bodies move along geodesics, while gravitational waves perturb space-time as they propagate. The mass quadrupole moment is the lowest order contribution to GW emission, in case its second time derivative is non-zero.

The main idea behind a space-based GWO is to consider two free falling masses travelling on their own geodesic, whose relative distance changes when a gravitational wave passes through. Therefore, a space-based observatory shall be primarily equipped with two devices:

- a drag-free and attitude control system (DFACS), which compensates for all the non-gravitational disturbances and guarantees free-fall conditions;
- a laser interferometer, which measures the relative optical path length.

Even if the DFACS works properly, the relative distance between TMs will change, due to different phenomena [1]:

- GWs, which cause picometric/nanometric deformations of the LISA constellation, with relative accelerations of few femto-m/s^2;
- orbital dynamics, which cause armlength variations (± 35.000 km) and μm/s^2 relative accelerations.

Fortunately, GWs' effects can be distinguished since orbital dynamics deformations occur at much lower frequencies (yearly variations) and can be ultimately predicted.

GW tidal deformations introduce length variations of the optical path between each two TMs; to be detected via laser interferometry as a time-varying Doppler shift of the light frequency.

As a result, two noise sensitivity functions can be derived [1] as basis for the main AOCS requirements: the first one, S_a, is related to the single test mass acceleration noise and it is the main performance requirement for the DFACS. If this constraint is not fulfilled, the free-fall condition is no more guaranteed and so the resultant relative motion of the test masses

shadows the nanometric distance variations induced by gravitational waves along the measurement arm.

$$S_a^{1/2} \leq 3 \cdot 10^{-15} \frac{\text{ms}^{-2}}{\sqrt{\text{Hz}}} \sqrt{1+\left(\frac{0.4\,\text{mHz}}{f}\right)^2} \sqrt{1+\left(\frac{f}{8\,\text{mHz}}\right)^4}$$

$$0.02\ m\text{Hz} \leq f \leq 1\ Hz$$

The second strain sensitivity function, S_{IFO}, is related to the displacement noise and it is the main performance requirement for the laser interferometer.

$$S_{IFO}^{1/2} \leq 1 \cdot 10^{-11} \frac{\text{m}}{\sqrt{\text{Hz}}} \sqrt{1+\left(\frac{2\,\text{mHz}}{f}\right)^2}$$

$$0.02\ m\text{Hz} \leq f \leq 1\ Hz$$

3. Non-linear Modelling

In this section, an innovative non-linear mathematical model of the dynamics underlying the latest LISA mission concept is presented, as a path towards a new DFACS design. The model here presented was developed by also bearing in mind the control system design process. Specifically, the envisaged model-based DFACS will aim to satisfy LISA challenging requirements holistically, including TM release and constellation acquisition. Further, a special attention is devoted to disturbances, to be actively minimised or counteracted by the DFACS.

3.1 Mathematical Notations

- A generic reference frame is denoted with $\text{RF} = \left\{O, \vec{j}_1, \vec{j}_2, \vec{j}_3\right\}$, where O is the origin and $\left\{\vec{j}_1, \vec{j}_2, \vec{j}_3\right\}$ is a right-handed orthonormal basis in $\mathbb{R}^3$.

- A generic vector $\vec{r} \in \mathbb{R}^3$ can be expressed as $\sum_{i=1}^{n} r_i \vec{j}_i$, where $\left\{\vec{j}_k\right\}_{k=1}^{n}$ is an orthonormal basis in $\mathbb{R}^3$. The components of $\vec{r}$ can be collected in a so-called coordinate vector (denoted with the bold style) according to:

$$\mathbf{r} = (r_1, \ldots, r_n) = \begin{bmatrix} r_1 & \cdots & r_n \end{bmatrix} = \begin{bmatrix} r_1 \\ \vdots \\ r_n \end{bmatrix} \in \mathbb{R}^{n \times 1}.$$

- A generic matrix is written as

$$A = \begin{bmatrix} A_{11} & \cdots & A_{1m} \\ \vdots & \ddots & \vdots \\ A_{n1} & \cdots & A_{nm} \end{bmatrix} \in \mathbb{R}^{n \times m}.$$

- Euclidean norm: $|\mathbf{r}| = \|\mathbf{r}\| = \sqrt{\sum_i r_i^2}$.

- Cross product:

$$\mathbf{r} \times = \begin{bmatrix} 0 & -r_3 & r_2 \\ r_3 & 0 & -r_1 \\ -r_2 & r_1 & 0 \end{bmatrix}.$$

- Rotations, attitude kinematics and dynamics:
  - $\boldsymbol{\theta} = (\phi, \theta, \psi)$: Euler angle vector.
  - T_a^b: rotation matrix RFb → RFa; equivalently, coordinate transformation RFa → RFb.
  - Elementary rotations:

$$X(\phi) \doteq \begin{bmatrix} 1 & 0 & 0 \\ 0 & c\phi & -s\phi \\ 0 & s\phi & c\phi \end{bmatrix}, \quad Y(\theta) \doteq \begin{bmatrix} c\theta & 0 & s\theta \\ 0 & 1 & 0 \\ -s\theta & 0 & c\theta \end{bmatrix}, \quad Z(\psi) \doteq \begin{bmatrix} c\psi & -s\psi & 0 \\ s\psi & c\psi & 0 \\ 0 & 0 & 1 \end{bmatrix}$$

where $c = \cos$, $s = \sin$.
  - Rotation matrix as a function of Euler angles (Tait-Bryan 321):

$$T(\boldsymbol{\theta}) = Z(\psi) Y(\theta) X(\phi)$$
$$T^{-1}(\boldsymbol{\theta}) = X(-\phi) Y(-\theta) Z(-\psi).$$
  - Kinematic matrix (Tait-Bryan 321):

$$Q(\boldsymbol{\theta}) = \frac{1}{c\theta} \begin{bmatrix} c\theta & s\phi\,s\theta & c\phi\,s\theta \\ 0 & c\phi\,c\theta & -s\phi\,c\theta \\ 0 & s\phi & c\phi \end{bmatrix}, \quad \boldsymbol{\theta} = \begin{bmatrix} \phi \\ \theta \\ \psi \end{bmatrix}$$
  - Gyroscopic acceleration:

$$\boldsymbol{\Lambda}(\boldsymbol{\omega}) \equiv \boldsymbol{\Lambda}(\boldsymbol{\omega}, J) = -J^{-1} \boldsymbol{\omega} \times J \boldsymbol{\omega}.$$
  - Fictitious acceleration:

$$\boldsymbol{\Gamma}(\mathbf{r}, \boldsymbol{\omega}) \equiv \boldsymbol{\Gamma}(\mathbf{r}, \dot{\mathbf{r}}, \boldsymbol{\omega}, \dot{\boldsymbol{\omega}}) =$$
$$= -\dot{\boldsymbol{\omega}} \times \mathbf{r} - 2\boldsymbol{\omega} \times \dot{\mathbf{r}} - \boldsymbol{\omega} \times (\boldsymbol{\omega} \times \mathbf{r})$$
  - Rotation matrix derivatives:

$$\dot{T} = T\boldsymbol{\omega} \times$$
$$\ddot{T} = T\Omega, \quad \Omega = \boldsymbol{\omega} \times \boldsymbol{\omega} \times + \dot{\boldsymbol{\omega}} \times.$$

3.2 Reference Frames

- Inertial frame: $\text{IF} = \left\{O_I, \vec{I}_1, \vec{I}_2, \vec{I}_3\right\}$.
  - Origin O_I: Sun CoM.
  - Axes (unit vectors): $\left\{\vec{I}_1, \vec{I}_2, \vec{I}_3\right\}$, where the plane $\left\{\vec{I}_1, \vec{I}_2\right\}$ is equal to the ecliptic plane of the triangle center.
- Local constellation frame:
  $\text{CFi} = \left\{O_{Si}, \vec{c}_{1i}, \vec{c}_{2i}, \vec{c}_{3i} = \vec{c}_3\right\}$, where $i = 1, 2, 3$ is the S/C number.
  - Origin O_{Si}: S/C CoM.

- Axes (unit vectors): $\left\{\vec{c}_{1i},\vec{c}_{2i},\vec{c}_{3}\right\}$, where $\vec{c}_{1i}$ is the bisector of the two constellation arms starting from the S/C CoM.

- S/C frame: SFi = $\left\{O_{Si},\vec{s}_{1i},\vec{s}_{2i},\vec{s}_{3i}\right\}$, where $i=1,2,3$ is the S/C number.
  - Origin O_{Si}: CoM of S/Ci.
  - Axes (unit vectors): $\left\{\vec{s}_{1i},\vec{s}_{2i},\vec{s}_{3i}\right\}$, where $\left\{\vec{s}_{1i},\vec{s}_{2i}\right\}$ lies in the optical plane defined by the telescopes optical axis and $\vec{s}_{1i}$ is the bisector of the two telescopes optical axis.

- Optical assembly frame: OFji = $\left\{O_{Oji},\vec{o}_{1ji},\vec{o}_{2ji},\vec{o}_{3ji}\right\}$, where $i=1,2,3$ is the S/C number and $j=1,2$ is the OA number.
  - Origin O_{Oji}: CoM of OAji.
  - Axes (unit vectors): $\left\{\vec{o}_{1ji},\vec{o}_{2ji},\vec{o}_{3ji}\right\}$, where $\left\{\vec{o}_{1ji},\vec{o}_{2ji}\right\}$ are on the optical plane previously defined and $\vec{o}_{1ji}$ is the telescope optical axis. We assume that the axis $\vec{o}_{3ji}$ is orthogonal to the optical plane and thus parallel to $\vec{s}_{3i}$.

- Test mass frame: MFji = $\left\{O_{Mji},\vec{m}_{1ji},\vec{m}_{2ji},\vec{m}_{3ji}\right\}$, where $i=1,2,3$ is the S/C number and $j=1,2$ is the TM number (equal to the corresponding OA number).
  - Origin O_{Mji}: CoM of TMji.
  - Axes (unit vectors): $\left\{\vec{m}_{1ji},\vec{m}_{2ji},\vec{m}_{3ji}\right\}$, where $\vec{m}_{1ji}$ is orthogonal to the +x face of the TM and $\vec{m}_{3ji}$ is orthogonal to the +z face.

3.3 Non-linear Equations

The equations of motion for the various elements composing the LISA observatory are now reported. They are written for a generic S/C, OA, and TM. The indexes i (denoting the S/C) and j (denoting the OA and the TM) will be used only when necessary, otherwise they will be omitted. The equations have been derived by means of the Newton-Euler approach.

<u>S/C translation model:</u> The Newton's law for a generic S/C (including the two movable OAs and a movable antenna) of LISA can be written as:

$$\ddot{\mathbf{r}}_I = -\mu_\odot\frac{\mathbf{r}_I}{\left|\mathbf{r}_I\right|^3} + m_S^{-1}T_S^I\left(\mathbf{F}_T+\mathbf{d}_S\right) - m_S^{-1}\sum_{i=1,2}T_{Oi}^I\mathbf{F}_{Ei}.$$

The signal $\mathbf{d}_S$ accounts for environment forces, gravity anomalies, suspension and MPA noises.

<u>S/C rotation model:</u> The Euler's and kinematic equations for a generic S/C are written as

$$\dot{\boldsymbol{\omega}}_{SI} = \Lambda\left(\boldsymbol{\omega}_{SI}\right)+J_S^{-1}\left(\mathbf{M}_T-\ldots\right.$$

$$\left.\ldots-\sum_{l=1,2}\left(\left(\mathbf{b}_{Sl}+T_{Ol}^S\mathbf{b}_M\right)\times T_{Ol}^S\mathbf{F}_{El}+T_{Ol}^S\mathbf{M}_{El}\right)+\mathbf{D}_S\right)$$

$$\boldsymbol{\omega}_S = \boldsymbol{\omega}_{SI}-T_C^S\boldsymbol{\omega}_C$$

$$\dot{\boldsymbol{\theta}}_S = Q\left(\boldsymbol{\theta}_S\right)\boldsymbol{\omega}_S$$

where the signal $\mathbf{D}_S$ accounts for environment torques, actuator noise and variations of J_S. The subscript C refers to the local constellation frame of the current S/C.

<u>TM translation model:</u> The acceleration of the j-th TM of LISA, relatively to the cage center, is given by

$$\ddot{\mathbf{r}}_{Mj} = T_I^{Oj}\ddot{\mathbf{r}}_{Mj}^I-\Omega_{Oj}\mathbf{r}_{Mj}-2\boldsymbol{\omega}_{Oj}\times\dot{\mathbf{r}}_{Mj}$$

where

$$\ddot{\mathbf{r}}_{Mj}^I = \ddot{\mathbf{r}}_{MIj}-\ddot{\mathbf{r}}_I-T_S^I\Omega_{SI}\mathbf{b}_S-T_{Oj}^I\Omega_{Oj}\mathbf{b}_M$$

$$\ddot{\mathbf{r}}_{MIj} = -\mu_\odot\frac{\mathbf{r}_{MIj}}{\left|\mathbf{r}_{MIj}\right|^3}+m_M^{-1}T_{Oj}^I\left(\mathbf{F}_{Ej}+\mathbf{d}_{Mj}\right).$$

The signal $\mathbf{d}_{Mj}$ accounts for the MPA and suspension noises and environment forces. The derivation of these equations is not reported here for the sake of brevity.

<u>TM rotation model:</u> The Euler's and kinematic equations for the j-th TM of LISA can be written as:

$$\dot{\boldsymbol{\omega}}_{MIj} = \Lambda\left(\boldsymbol{\omega}_{MIj}\right)+J_M^{-1}\left(K_{Rj}\boldsymbol{\theta}_{Mj}+T_{Oj}^{Mj}\mathbf{M}_{Ej}+\mathbf{D}_{Mj}\right)$$

$$\boldsymbol{\omega}_{Mj} = \boldsymbol{\omega}_{MIj}-T_{Oj}^{Mj}\left(0,0,\dot{\zeta}_j\right)-T_S^{Mj}\boldsymbol{\omega}_{SI}$$

$$\dot{\boldsymbol{\theta}}_{Mj} = Q\left(\boldsymbol{\theta}_{Mj}\right)\boldsymbol{\omega}_{Mj}$$

where $K_{Rj}\boldsymbol{\theta}_{Mj}$ is a stiffness term, including all moments proportional to the angular displacement of the MF with respect to the OF. The signal $\mathbf{D}_{Mj}$ accounts for environment torques and suspension noise.

<u>OA rotation model:</u> A simple first-order model is considered for the OA rotation motion, given by

$$\dot{\zeta}_j = c_{OA}u_{OAj}+d_{\zeta j}$$

where $d_{\zeta j}$ represents the OA motor noise. A more detailed model could be developed, but this is deemed adequate to capture the relevant behaviors of the OA dynamics.

Micro-propulsion actuators: As a baseline, MPAs can be modelled by second-order dynamics accompanied by a delay. Thrust noise and bias can be added to the dynamic output. The input is quantized and saturated being the output of a DAC. In this preliminary study, a simplified noise-free static model is considered:

$$\begin{bmatrix} \mathbf{F}_T \\ \mathbf{M}_T \end{bmatrix} = \begin{bmatrix} B_{TF} \\ B_{TM} \end{bmatrix} \mathbf{u}_T$$

where $B_{TF}, B_{TM} \in \mathbb{R}^{3 \times 9}$ are matrices defined on the basis of the thruster assembly geometry [19].

Electrostatic suspension: The suspension model aims to express electrostatic forces in terms of TM position and attitude fluctuations $(\mathbf{r}_M, \boldsymbol{\theta}_M)$ with respect to the optical frame. The noise-free expressions that we consider is the following:

$$\begin{bmatrix} \mathbf{F}_E \\ \mathbf{M}_E \end{bmatrix} = \begin{bmatrix} A_{EF} & A_{MF} \\ A_{FM} & A_{EM} \end{bmatrix} \begin{bmatrix} \mathbf{r}_M \\ \boldsymbol{\theta}_M \end{bmatrix} + \begin{bmatrix} B_{EF} & B_{MF} \\ B_{FM} & B_{EM} \end{bmatrix} \begin{bmatrix} \mathbf{u}_{EF} \\ \mathbf{u}_{MF} \end{bmatrix}$$

where $A_{EF}, A_{EM}, A_{FM}, A_{MF} \in \mathbb{R}^{3 \times 3}$,

$B_{EF}, B_{EM}, B_{FM}, B_{MF} \in \mathbb{R}^{3 \times 3}$, and $\mathbf{u}_E = (\mathbf{u}_{EF}, \mathbf{u}_{EM})$ is the vector of the digital suspension commands. The state and control matrices are function of the electrodes' characteristics (i.e. capacitances, voltages, gaps, surfaces, arms). Specifically, $A_{FM}, A_{MF}, B_{FM}, B_{MF}$ describe the cross-coupling effects.

4. LISA DFAC Unit
In this section, a general overview of the the most relevant control solutions and architectures adopted within LISA past studies are discussed and traded-off, with a special attention given to the Embedded Model Control (EMC) methodology, together with the LISA DFACS chief design principles.

4.1 Control Design Principles
For what concerns degrees of freedom, a LISA S/C is characterised by 19 DoFs:

- 7 DoFs for each S/C:
  - 3 linear positions (actuated for drag-free purposes but not for constellation control),
  - 3 attitude angles (actuated);

- 1 angle between the OA axes (actuated).

- 12 DoFs for each pair of TMs:
  - 6 linear positions (actuated);
  - 6 attitude angles (actuated).

During the science measurement phase, the 6 TM positions are arranged into 3 drag-free coordinates (2 longitudinal and the mean vertical coordinate of the TM pair) and 3 suspension coordinates (2 lateral and the difference between the vertical coordinates). The 3 DF coordinates are actuated together with the S/C attitude by the 9 thrusters of the Micro Propulsion Assembly (MPA). On the other hand, the 3 suspension coordinates are actuated by 4 suspension actuators. A pair of actuators actuates the vertical difference.

Table 1 summarizes the DoFs and the related sensors and actuators. Star trackers are not used during Science Mode since they are too noisy, especially at low frequencies, as demonstrated by LPF ([2], [3]).

DoF	Sensor	Actuator
S/C CoM position	N/A	No constellation control
S/C attitude	STR	MPS
S/C attitude (Science Mode)	OMS	MPS
OA inter-angle	ITS	ITA
TM attitude	GRS/OMS	GRS
TM position	GRS	GRS

Table 1. LISA S/C: DoFs, sensors and actuators

Given the latest LISA concept, the AOCS requirements, and the need for a wide-frequency drag-free control, also accounting for the several external disturbances, the driving principles for the DFACS design, during the science measurement phase, are:

1) *S/C attitude and TM drag-free control* (6 DoFs, 6 SISO systems, 12 controllable state variables, ≥ 6 disturbance state variables).
The drag-free control must be endowed with the widest BW possible, yet accounting for the thrusters and sensors neglected dynamics. The main control objectives are: (i) to accurately align the SF to the CF, and (ii) to abate the fluctuations S/C-to-TM along the drag-free axes.

2) *Lateral and vertical difference suspension, TM attitude control* (9 DoFs, 9 SISO systems, 18 state variables, ≥ 9 disturbance state variables).
The first aim of the suspension attitude control is to accurately align each TM to the incoming laser

beam direction, which defines the target drag-free axis. The second aim is to guarantee that the parasitic effect of the actuated electrostatic accelerations and torques (5 DoF) on the drag-free axis is compatible with LISA severe requirements.

3) *OA control system.* The contribution of the OA acceleration is preliminarily considered as completely accounted for by the unknown disturbance of S/C attitude and TM equations. As already remarked, the S/C residual acceleration may contribute to the OA acceleration, together with the motor noise. In fact, more in-depth analyses will assess the most relevant contributors to the final LISA performance, as well as the best modelling or mitigation strategies.

4.2 DFACS for the Science Mode

All the Science Mode control systems rely on input-output decoupling, to reduce the control of the original MIMO system into a set of simple SISO tasks design. Such an approach yields an extended insight into the system and physical design constraints, which can easily be identified. In turn, the original drag-free and pointing requirements were re-formulated in terms of closed loop frequency response specifications. Consequently, different control techniques can be applied.

Three principal drivers were established to select the control techniques to be reviewed and traded-off for a new LISA DFACS design: (i) LISA PF heritage, (ii) the methodologies better fitting the overall LISA requirements (in all mission phases), and (ii) the previous LISA studies and experiences.
Concerning LISA PF, it is undisputable that its heritage and in-flight experience will provide a compelling perspective into the selection and the derivation of the control design architecture for LISA.
In addition, the latest trade-offs and solutions, both at mission and satellite level, seem to lead the control design mainly to: (i) H-infinity techniques, and (ii) robust model-based designs, as the Embedded Model Control (EMC). Specifically, if the former approach allows an optimization of the spectral density performance based on the given requirements, the latter one relies upon a disturbance-rejection-based rationale.
Finally, it might be of interest to build also on the heritage and lessons learnt provided by other established approaches, as Sliding Mode Control and Mu-synthesis.

4.2.1 A Pathfinder Perspective
Free Fall / Drift (TESTED in-flight by LPF) [4],[5]
To assess the acceleration noise acting on it due to the suspension control, LPF performed the Free-fall (or Drift) Mode control. In this mode, the suspension system is turned ON and OFF with a low duty cycle (about 1 s OFF-time). In this way, the actuation is

limited to brief kicks, so that the second TM is in free fall between two successive kicks. The actuation-free motion is then analyzed for the remaining sources of acceleration noise. In fact, this mode solves, at least partially, the problem of the actuation noise, as the φ (angular rotation around z-axis) control remains. The LPF free-fall experiment constitutes an alternative technique for measuring the differential TM acceleration without the added force noise and calibration issues introduced by the actuator. On the other hand, both the φ residual noise and difficulties in discarding the kicks for data analysis, made the final performance level, in Drift Mode, comparable to the one achieved in the LPF main Science Mode.

Proportional-Integral-Derivative (PID) with roll-off filters (TESTED in-flight by LPF) [6]
PID controllers with inclusion, especially for drag-free, of lead and lag compensators and 4th-order attenuation filters were used to perform the different SISO controllers. Promising in-flight results have been obtained by DRS, during LPF mission. Indeed, the DRS has met all its position accuracy and drag-free requirements, as well as the goal on test mass residual accelerations within the MBW, with significant margins. The noise performance, in general, was substantially better than expected, mainly due to the LTP and the thrusters outperforming their requirements.

4.2.2 Modern Robust Control Solutions
H-infinity (H∞) (TESTED in-flight by LPF) [7-15]
The use of the H∞ design technique allowed an optimization of the spectral density performance. Indeed, based on the requirements given for the different controlled axes, further requirements for the sensitivity functions were derived and checked for consistency and physical infeasibilities. This technique has been successfully also used in the LPF DFACS. From switch-on to extended mission operations, LPF DFACS worked in agreement with the requirements. However, this preliminary success has been made possible by several and in-depth studies about the LTP system, during its development and implementation phases.

Embedded Model Control, disturbance-rejection-based approach (TESTED in-flight by GOCE) [18],[19]
The Embedded Model Control allows proceeding systematically from fine plant dynamics and controlling requirements to the Embedded Model (EM), which is the core of control design and algorithms. The model defines three interconnected parts: the controllable dynamics, the disturbance class to be rejected and the neglected dynamics. Control algorithms are designed around the first two parts (the controllable dynamics and the disturbance estimation dynamics), while stability

and performance are constrained by the third one. The key design issue is discriminating between driving noise and neglected dynamics, to guarantee updating disturbance in view of its rejection. Hence, one main problem is the disturbance rejection, with the notion of disturbance representing the uncertainties, both internal and external to the plant.

4.2.3 *Past LISA Studies Heritage*
Sliding Mode Control (TESTED in-flight by LPF, for TM release) [16],[17]
A systematic approach to the problem of achieving stability and consistent performance against consistent modelling imprecisions. It is based on a simple approach to robust control, able to deal with several model uncertainties, forcing ideally a non-linear and high-order plant to behave as a first or second order system. With an accurate control law design, it is possible to trade-off among admissible control activity to achieve a good compromise between control performance and parametric uncertainty.

Mu-synthesis [7],[9]
Leveraging uncertain state-space models, μ-synthesis based controllers optimize the structured singular value to obtain robust performances in the case of dynamic structured, and parametric uncertainty. To this aim, control system decoupling, and frequency performance analysis, provided also a relevant feedback, at system perspective. Indeed, areas where the system and control requirements might be relaxed were highlighted, as well as the required TM readout noise levels were suitably identified.

5. Conclusions
In summary, we have presented an outline of the mission design and requirements for the future LISA gravity wave space mission, under study by ESA. This design was based on the heritage of the LISA Pathfinder mission.
A non-linear model of the LISA complete dynamics was developed as a basis for a novel drag-free and attitude control unit design, with the aim to satisfy LISA challenging requirements holistically, including TM release and constellation acquisition.
Finally, the preliminary control design principles were outlined, in parallel with the most promising control solutions and architectures. Specifically, the architecture selection took into account the LISA PF heritage, the overall LISA requirements, in all mission phases, and the systematic review of the previous studies and experiences.

Acknowledgements

References
[1] Danzmann, K., et al., "LISA Laser Interferometer Space Antenna: a proposal in response to the ESA call for L3 mission concepts", Albert Einstein Institute Hannover, Leibniz Universität Hannover and Max Planck Institute for Gravitational Physics, 20 January 2017

[2] Schleicher, A., et al., "In-Orbit performance of the LISA PathFinder Drag Free and Attitude Control System", *GNC 2017: 10th International ESA Conference on Guidance, Navigation and Control Systems*, Salzburg, Austria, 29 May – 2 June 2017

[3] M. Armano et al., "Beyond the Required LISA Free-Fall Performance: New LISA Pathfinder Results down to 20 μHz", Phys. Rev. Lett. 120, 061101, 2018

[4] R. Giusteri et al., The free-fall mode experiment on LISA Pathfinder: first results, Journal of Physics Conf. Series 840 012005, 2017

[5] J. Conklin et al., Drift mode accelerometry for spaceborne gravity measurements, 2014.

[6] P. G. Maghami et al., Drag-Free Performance of the ST7 Disturbance Reduction System Flight Experiment on the LISA Pathfinder, System, Proceedings of the 10th International ESA Conference on Guidance Navigation & Control Systems, 29 May – 2 June 2017, Salzburg, Austria, 2017

[7] H. Klotz, Drag-free, Attitude and orbit control for LISA, 3rd SGNCS ESTEC Noordwijk, 26-29 November, 1996

[8] P. F. Gath, U. Johann, H.R. Schulte, D. Weise, M. Ayre, 2006, November. LISA system design overview. In AIP conference proceedings (Vol. 873, No. 1, pp. 647-653). AIP

[9] P. F. Gath et al., Drag Free and Attitude Control System Design for the LISA Science Mode, Proceedings of the AIAA Guidance, Navigation and Control Conference and Exhibit, 20 - 23 August 2007, Hilton Head, South Carolina, 2007

[10] W. Fichter et al., Closed Loop Performance and Limitations of the LISA Pathfinder Drag-Free Control System, Proceedings of the AIAA Guidance, Navigation and Control Conference and Exhibit, 20 - 23 August 2007, Hilton Head, South Carolina, 2007

[11] W. Fichter et al., LISA Pathfinder drag-free control and system implications, Classical and Quantum Gravity, 22 S139-S148, 2005

[12] W. Fichter et al., Control tasks and functional architecture of the LISA Pathfinder drag-free system, Proceedings of the 6th International ESA

Conference on Guidance Navigation & Control Systems, 17 – 20 October 2005, Loutraki, Greece, 2005

[13] P. Gath, D. Weise, H.R. Schulte, and U. Johann, 2009. LISA mission and system architectures and performances. In Journal of Physics: Conference Series (Vol. 154, No. 1, p. 012013). IOP Publishing

[14] W. Fichter et al., Drag-Free Control Design with Cubic Test Masses, Published by Springer in Laser, Clocks & Drag Free Control book, 2008

[15] R. Saage, Closed Loop Specifications of Spacecraft Control Under Micro-Propulsion Constraints, Journal of Guidance, Control and Dynamics, Vol 35, No 5, 2012

[16] T. T. Hyde et al., Precision pointing for the laser interferometry space antenna mission, AAS-03-066, 2003

[17] P. G. Maghami et al., Laser interferometer space antenna dynamics and controls model, Classical and Quantum Gravity, 20 S273-S282, 2003

[18] E. Canuto, Drag-free and attitude control for the GOCE satellite, Automatica, 44(7) 2008 1766-1780

[19] E. Canuto, L. Colangelo, M. A. Lotufo, S. Dionisio, Satellite-to-satellite attitude control of a long-distance spacecraft formation for the Next Generation Gravity Mission, European Journal of Control, Volume 25, September 2015, Pages 1-16, ISSN 0947-3580

[20] Laser Interferometer Gravitational Wave Observatory, https://www.ligo.caltech.edu/, (accessed 15.09.18).

[21] http://www.virgo-gw.eu/, (accessed 15.09.18).

[22] L. Massotti, E. Canuto, and P. Silvestrin, 2006, June. Embedded Model Control Application to Drag-Free and Satellite-to-Satellite Tracking. In Control and Automation, 2006. MED'06. 14th Mediterranean Conference on (pp. 1-6). IEEE

[23] D. Bortoluzzi, M. Da Lio, R. Oboe, and S. Vitale, 2004, March. Spacecraft high precision optimized control for free-falling test mass tracking in LISA-Pathfinder mission. In The 8th IEEE International Workshop on Advanced Motion Control, 2004. AMC'04. (pp. 553-558). IEEE

[24] M. Armano, H. Audley, G. Auger, J.T. Baird, M. Bassan, P. Binetruy, M. Born, D. Bortoluzzi, N. Brandt, M. Caleno, and L. Carbone, 2016. Sub-femto-g free fall for space-based gravitational wave observatories: LISA pathfinder results. Physical review letters, 116(23), p.231101

[25] S. Vitale, 2014. Space-borne gravitational wave observatories. General Relativity and Gravitation, 46(5), p.1730

[26] D. Bortoluzzi, D., et al., 2016. Injection of a Body into a Geodesic: Lessons Learnt from the LISA Pathfinder Case

[27] L. Wissel, and LPF collaboration, 2017, May. LISA Pathfinder: Understanding DWS noise performance for the LISA mission. In Journal of Physics: Conference Series (Vol. 840, No. 1, p. 012044). IOP Publishing

[28] S.F. Wu, and D. Fertin, 2008. Spacecraft drag-free attitude control system design with quantitative feedback theory. Acta Astronautica, 62(12), pp.668-682

[29] G. E. Piper and J. M. Watkins, Investigating the control design of the disturbance reduction system for the LISA mission, in IEE Proceedings - Control Theory and Applications, vol. 153, no. 1, pp. 29-36, 16 Jan. 2006

[30] O. Jennrich, 2009. LISA technology and instrumentation. Classical and Quantum Gravity, 26(15), p.153001

[31] M. Sallusti, P. Gath, D. Weise, M. Berger, and H.R. Schulte, 2009. LISA system design highlights. Classical and Quantum Gravity, 26(9), p.094015